Optical characteristics of one-dimensional Si/SiO_2 photonic crystals for thermophotovoltaic applications

Francis O'Sullivan, Ivan Celanovic,[a] Natalija Jovanovic, and John Kassakian
Laboratory for Electromagnetic and Electronic Systems, Department of Electrical Engineering and Computer Science, Massachusetts Institute of Technology, Cambridge, Massachusetts 02139

Shoji Akiyama and Kazumi Wada
Department of Materials Science and Engineering, Massachusetts Institute of Technology, Cambridge, Massachusetts 02139

(Received 30 August 2004; accepted 17 November 2004; published online 19 January 2005)

This article presents a detailed exploration of the optical characteristics of various one-dimensional photonic crystal structures designed for use as a means of improving the efficiency and power density of thermophotovoltaic (TPV) devices. The crystals being investigated have a ten-layer quarter-wave periodic structure, and are based on Si/SiO_2 and Si/SiON material systems. For TPV applications the crystals are designed to act as filters, transmitting photons with wavelengths below 1.78 μm to a GaSb photodiode, while reflecting photons of longer wavelengths back to the source of thermal radiation. In the case of the Si/SiO_2 structure, the Si and SiO_2 layers were designed to be 170 and 390 nm thick, respectively. This structure was fabricated using low-pressure chemical vapor deposition. Reflectance and transmittance measurements of the fabricated Si/SiO_2 photonic crystals were taken from 0.8 to 3.3 μm for both polarizations and for a range of incident angles. Measurement results were found to correlate well with simulation results for the ideal structure. Measurement results were used to predict the TPV system efficiency, power density and spectral efficiency using an ideal thermodynamic model of a TPV system. © *2005 American Institute of Physics*. [DOI: 10.1063/1.1849437]

I. INTRODUCTION

Thermophotovoltaics (TPVs) convert thermal radiation emitted from a high-temperature source into electricity by means of a photovoltaic (PV) diode, as solar photovoltaic systems convert solar radiation into electricity.[1,2] Two of the major differences between TPV systems and solar power conversion systems are: (1) the thermal radiation source in TPV systems is in close proximity to the PV diode, and (2) the temperature of the emitter in the TPV system, typically in the 1100–1500 K range, is much lower than that of the sun. The lower source temperature demands that in order to obtain respectable system efficiency and power density, the PV diodes in a TPV system need to be fabricated from low band gap materials, e.g., GaSb, InGaAs, InGaAsSb. The close proximity of the thermal source to the PV diode (large view factor) also results in omnidirectional radiative power transfer and large incident radiative flux density. Fortunately, the close proximity also allows for photon "recycling," which can be used to significantly improve the overall system efficiency. The overall system efficiency and power density can be significantly enhanced by reflecting back to the emitter photons whose energies are below the electronic band gap energy (E_{gap}) of the PV diode, while transmitting photons whose energies are greater than E_{gap} to the PV diode to be converted into electricity.[2] Such energy recycling can be achieved through the use of either front-side filter structures (filter deposited on the front side of the PV diode) and/or backside reflectors (deposited on the backside of the PV diode).

This article investigates the use of one-dimensional (1D) photonic crystals as front-side filters for improving TPV system efficiency and power density. Within this context, the fundamental limitations of such structures are discussed, along with issues relating to the design, fabrication and optical characterization of the structures.

In recent years 1D photonic crystals designed as omnidirectional mirrors (made from a range of different material systems) have been studied extensively[3,4] for a range of applications in photonics and optoelectronics. Among the different candidate materials that have been studied for use in 1D photonic crystals, the Si/SiO_2 material system stands out. Its advantages include having a large dielectric index contrast, and the fact that numerous technologies exist for the fabrication of devices based on Si and SiO_2. However, most of the published material regarding the use of the Si/SiO_2 pair focuses on the omnidirectional stop-band characteristics, and the use of such photonic crystals as perfect mirrors.[4,5] There has been very little work carried out on the characterization of 1D photonic crystals serving as near-infrared omni-directional high-pass filters, which is effectively what these crystals are used for in TPV systems. Therefore, this article focuses on the pass- and stop-band characteristics of 1D photonic crystals in the near-infrared wavelength range

[a]Electronic mail: ivanc@mit.edu

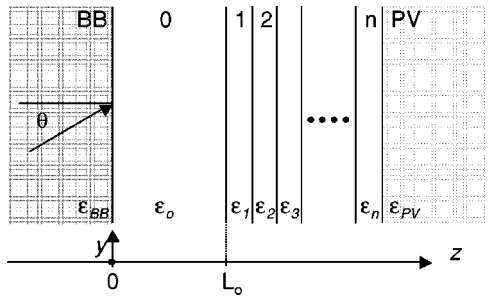

FIG. 1. TPV system with a front-side dielectric stack filter (layers 1 to n). The thickness of the gap (layer 0) between the emitter (BB) and the dielectric stack is L_o. The PV diode extends to $+\infty$.

(0.8–3.3 μm), at both normal and grazing angles of incidence. The influence in terms of efficiency and power density of these spectral characteristics on the overall TPV system performance is also investigated.

This article is organized in six sections. The second section introduces the thermodynamic model of a TPV system and defines the spectral efficiency of a filter. The PV diode efficiency, power density and filter spectral efficiency are then used as metrics for quantifying the advantages and disadvantages of different filter designs. The third section briefly introduces photonic crystal modeling, projected photonic band diagrams, filter design techniques, and the design trade-offs as they apply to a specific TPV system. The fourth section discuses the fabrication, while the fifth section details spectral performance characterization of a Si/SiO_2 based photonic crystal filter. The final section presents experimental results, compares the performance of existing filter designs, and investigates the projected efficiencies of TPV systems using the fabricated filter.

II. THERMOPHOTOVOLTAIC SYSTEM MODELING

In this article a TPV system is defined as consisting of a thermal emitter separated from a PV diode by a gap of length L_0. A 1D photonic crystal is placed on the front side of the diode, as shown in Fig. 1. The emitter is a blackbody source with refractive index n_{BB}. The diode is fabricated from GaSb and has an electronic band gap $E_{gap}=0.7$ eV (corresponding to a wavelength of $\lambda_{gap}=1.78$ μm and a refractive index $n=3.9$. The role of the 1D photonic crystal deposited on the front side of the PV diode is to transmit all the photons with energies above E_{gap} to the diode, while reflecting all the photons with energies below E_{gap} back to the emitter.

The amount of electrical power generated by the TPV system as well as the efficiency can be calculated using the ideal thermodynamic model.[6,7] The ideal thermodynamic model assumes that the PV diode material is an ideal semiconductor material where an incident photon with energy $\hbar\omega$ generates an electron hole pair if $\hbar\omega > E_g$. The losses that are modeled are radiative recombination losses, thermalization losses, and bellow-band gap energy photon absorption. Since the emitter is a blackbody at temperature T_{BB}, the amount of power radiated to the photodiode can be expressed as

$$P_{rad} = \int_0^{\infty}\int_0^{\theta_1} \frac{n_{BB}^2\omega^2}{(2\pi)^2c^2}\frac{\hbar\omega}{\exp\left(\frac{\hbar\omega}{kT_{BB}}\right)-1} \times T_{13}(\omega,\theta)\cos\theta\sin\theta d\theta d\omega - \int_{\omega_g}^{\infty}\int_0^{\theta_3} \frac{n_{PV}^2\omega^2}{(2\pi)^2c^2}\frac{\hbar\omega}{\exp\left(\frac{\hbar\omega - eV}{kT_{PV}}\right)-1} \times T_{31}(\omega,\theta)\cos\theta\sin\theta d\theta d\omega \quad (1)$$

Here c is the speed of light, $\hbar$ is Planck's constant normalized by 2π, k is Boltzmann's constant, T_{PV} is the temperature of the diode, n_{BB} and n_{PV} are the blackbody and diode refractive indices, respectively, $T_{13}(\omega,\theta)$ is the sum of the TE and TM mode transmittances from the blackbody to the PV diode, $T_{31}(\omega,\theta)$ is the sum of the TE and TM mode transmittances from the PV diode to the blackbody, θ is the incident angle of radiation from the blackbody source (see Fig. 1), $\theta_1=\arcsin(n_{PV}/n_{BB})$ for $n_{PV}<n_{BB}$ and $\theta_1=\pi/2$ otherwise, $\theta_3=\arcsin(n_{BB}/n_{PV})$ for $n_{PV}>n_{BB}$ and $\theta_3=\pi/2$ otherwise. The first term in Eq. (1) represents the total power transferred from the blackbody to the PV diode, while the second term represents the power re-radiated from the photodiode back to the emitter (radiative recombination losses). This equation can be rewritten as follows:

$$P_{rad} = \int_0^{\infty} \frac{n_{BB}^2\omega^2}{(2\pi)^2c^2}\frac{\hbar\omega}{\exp\left(\frac{\hbar\omega}{kT_{BB}}\right)-1}\overline{T_{13}}(\omega)d\omega - \int_{\omega_g}^{\infty} \frac{n_{PV}^2\omega^2}{(2\pi)^2c^2}\frac{\hbar\omega}{\exp\left(\frac{\hbar\omega - eV}{kT_{PV}}\right)-1}\overline{T_{31}}(\omega)d\omega, \quad (2)$$

where

$$\overline{T_{xy}}(\omega) = \int_0^{\theta_x}\{T_{xyTE}(\omega,\theta) + T_{xyTM}(\omega,\theta)\}\cos\theta\sin\theta d\theta \quad x,y \in \{1,3\} \quad (3)$$

T_{xyTE} and T_{xyTM} are the TE and TM mode transmittances, respectively, and are functions of the frequency ω, angle of incidence θ and the gap length L_0. As defined, $\overline{T_{13}}$ is interpreted as the average transmittance from the emitter to the diode, and is the key to shaping the power transfer within a TPV system. Similarly, $\overline{T_{31}}$ is the average transmittance from the diode to the emitter.

The total electrical power generated in the photodiode is calculated as the product of the voltage (V) across the PV diode terminals, the electron charge (e), and the difference between the absorbed photon flux and reradiated photon flux. This can be conveniently expressed as

$$P_{\mathrm{PV}} = \mathrm{eV}\left\{\int_{\omega_g}^{\infty} \frac{n_{\mathrm{BB}}^2\omega^2}{(2\pi)^2c^2}\frac{1}{\exp\left(\frac{\hbar\omega}{kT_{\mathrm{BB}}}\right)-1}\overline{T_{13}}(\omega)d\omega - \int_{\omega_g}^{\infty} \frac{n_{\mathrm{PV}}^2\omega^2}{(2\pi)^2c^2}\frac{1}{\exp\left(\frac{\hbar\omega-\mathrm{eV}}{kT_{\mathrm{PV}}}\right)-1}\overline{T_{31}}(\omega)d\omega\right\}. \quad (4)$$

Again, the first term in Eq. (4) is the photon flux from the blackbody to the PV diode while the second term is the photon flux reradiated from PV cell to the blackbody (radiative recombination losses). TPV efficiency is defined using Eq. (2) and Eq. (4) as follows:

$$\eta_{\mathrm{TPV}}(T_{\mathrm{BB}},\omega_g,T_{\mathrm{PV}},V) = \frac{P_{\mathrm{PV}}(T_{\mathrm{BB}},\omega_g,T_{\mathrm{PV}},V)}{P_{\mathrm{rad}}(T_{\mathrm{BB}},\omega_g,T_{\mathrm{PV}},V)}. \quad (5)$$

From Eqs. (2)–(5) it is clear that power density and efficiency levels are strongly influenced by $\overline{T_{13}}$, and that by tailoring $\overline{T_{13}}$, superior system performance can be achieved.

In this article the performance of photonic crystal components is characterized with respect to PV diode power density given by Eq. (4), and diode efficiency according to Eq. (5). In addition, the filter's spectral efficiency is used as a figure of merit for the filter's performance. Spectral efficiency for a blackbody source is defined as[2]

$$\eta_{\mathrm{spectral}}(T_{\mathrm{BB}},\omega_g) = \frac{\int_0^{\omega_g} \frac{n_{\mathrm{BB}}^2\omega^2}{(2\pi)^2c^2}\frac{\hbar\omega}{\exp\left(\frac{\hbar\omega}{kT_{\mathrm{BB}}}\right)-1}\overline{T_{13}}(\omega)d\omega}{\int_0^{\infty} \frac{n_{\mathrm{BB}}^2\omega^2}{(2\pi)^2c^2}\frac{\hbar\omega}{\exp\left(\frac{\hbar\omega}{kT_{\mathrm{BB}}}\right)-1}(1-\overline{R_{13}}(\omega))d\omega}. \quad (6)$$

Here $\overline{T_{13}}(\omega)$ is the average transmittance of the filter as defined in Eq. (3), while $\overline{R_{13}}(\omega)=1-\overline{T_{13}}(\omega)$, neglecting the absorption losses in the filter in the wavelength range of interest. Spectral efficiency gives the ratio of the transmitted power above the band gap energy to the total emitted power that reaches the PV diode-filter system. Ideally the 1D photonic crystal would transmit all the photons above E_{gap} to the PV diode ($\overline{T_{13}}=1$ for $\omega>\omega_{\mathrm{gap}}$), and reflect all the lower energy photons back to the emitter ($\overline{T_{13}}=0$ for $\omega<\omega_{\mathrm{gap}}$). This performance would result in unity spectral efficiency over the entire frequency range, but still an the overall system efficiency [as defined by Eq. (5)], of less than one because the TPV system efficiency with GaSb PV diode is less than ideal [61% at maximum power point for GaSb diode at $T_{\mathrm{BB}}=1500\ K$ and $T_{\mathrm{PV}}=300\ K$, Eqs. (2)–(5)]. Although achieving ideal spectral control is not possible using 1D photonic crystals, this article will show that the use of a multiperiod Si/SiO_2 structure, deposited directly on the front side of the PV diode using low-pressure chemical vapor deposition (LPCVD), can provide impressive if not ideal spectral control. It will also be shown that basic modifications to the periodic structure of the crystal can further enhance the crystal's pass-band performance.

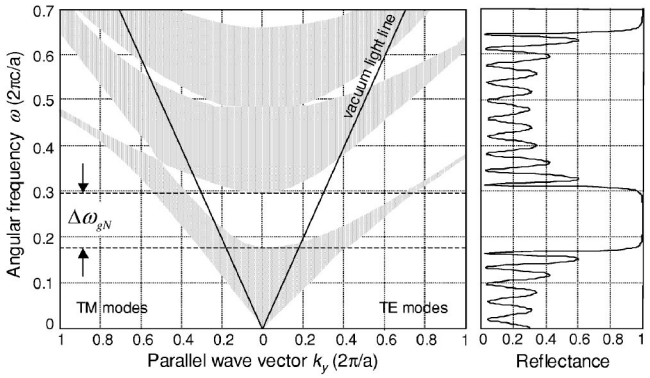

FIG. 2. Projected photonic band diagram for one-dimensional Si/SiO_2 quarter-wave stack for both polarizations (left) and reflectance at normal incidence of six pair Si/SiO_2 PhC deposited on Si substrate (right). Light line represents $\omega=1/\sqrt{\mu\epsilon}k_y$. Normal incidence band gap is designated as $\Delta\omega_{gN}$.

III. MODELING AND DESIGN OF 1D SI/SIO_2 PHOTONIC CRYSTALS

In order to gain more insight into the mechanisms relating power transfer from the blackbody source to the photonic crystal deposited on the diode (as in Fig. 1), the photonic band gap diagram of an infinite 1D photonic crystal will be analyzed. The projected photonic band diagram of an infinite 1D photonic crystal composed of alternating layers of Si and SiO_2 is given in Fig. 2, and is calculated using the transfer matrix method. The propagating electromagnetic modes are represented by the shaded regions, while the white regions represent nonpropagating modes. Although the 1D photonic crystal does not exhibit a full band gap, when coupled to free space the crystal can exhibit total omnidirectional reflectance.[8] For omnidirectional reflection to occur there must be no overlap between the projected photonic crystal's propagating bands and the projected free space propagating bands, over a certain frequency range. The projected band structure for free space is the cone above the light line characterized by $\omega^2=1/(\mu\varepsilon)(k_y^2+k_z^2)$. It is obvious from Fig. 2 that there exists a band of frequencies for which there is no overlap between the free space modes and the photonic crystal modes. This band gap is used to design the TPV filter. By aligning the upper edge of the normal incidence band gap (denoted as ω_{gap}) with the electronic band gap of the diode λ_g (1.78 μm for GaSb), the photonic crystal will reflect almost all the photons with frequencies in the range $(\omega_{\mathrm{gap}},\omega_{\mathrm{gap}}+\Delta\omega_{gN})$ where $\Delta\omega_{gN}$ is the normal incidence photonic band gap. Since the width of the first band gap is given as:[9]

$$\Delta\omega_{gN} = \omega_0\frac{4}{\pi}\sin^{-1}\frac{n_2-n_1}{n_2+n_1}, \quad (7)$$

where ω_0 is the central frequency of the band gap, it is easy to express this equation in terms of the band gap central wavelength (λ_0) and the band gap width (λ_g) as

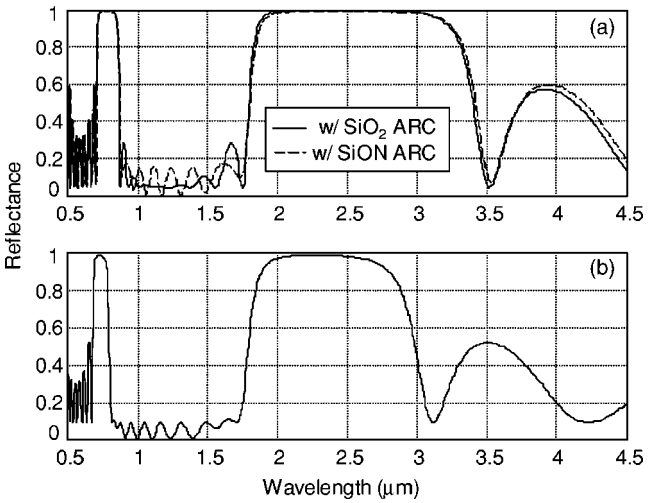

FIG. 3. Normal incidence reflectance for (a) Si/SiO_2 photonic crystal with SiO_2 ARC and SiON ARC (b) Si/SiON $L/2H(LH)^4$ photonic crystal.

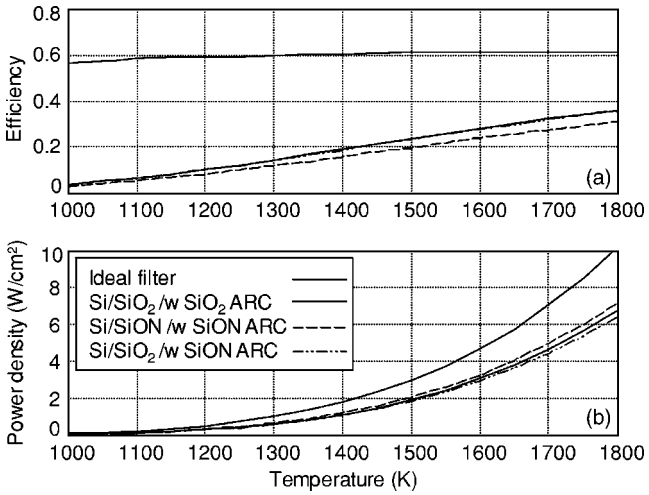

FIG. 4. Simulated system efficiency and power density of GaSb TPV system vs the emitter temperature with an ideal filter, Si/SiO_2 $L/2H(LH)^4$ photonic crystal, Si/SiON $L/2H(LH)^4$ and Si/SiO_2 photonic crystal with SiON ARC.

$$\lambda_0 = \frac{1}{2}\left(1 + \frac{2 + \frac{4}{\pi}\sin^{-1}\frac{n_2 - n_1}{n_2 + n_1}}{2 - \frac{4}{\pi}\sin^{-1}\frac{n_2 - n_1}{n_2 + n_1}}\right)\lambda_g. \tag{8}$$

Since the 1D photonic crystal filter is based on a quarter-wave dielectric stack, the thickness of the Si and SiO_2 layers is related by

$$\lambda_0 = 4n_1d_1 = 4n_2d_2, \tag{9}$$

where n_1 and d_1 represent the refractive index and thickness of the SiO_2 layer, and n_2 and d_2 represent the refractive index and thickness of the Si layer. In this case $n_1 = 1.5$, $d_1 = 0.39$ μm, $n_2 = 3.4$, and $d_2 = 0.17$ μm. The deposited structure is a ten-layer 1D photonic crystal, described as (LH),[5] where L and H represent quarter-wavelength thick layers of SiO_2 (low refractive index) and Si (high refractive index), respectively, starting from free space and ending at the PV diode as shown in Fig. 1.

The normal incidence reflectance of the structure deposited on a Si substrate is given in Fig. 2. Here the photonic crystal filter's stop band is clearly evident. However, large oscillations in the pass band ($\omega > \omega_{gap}$) significantly reduce the amount of power transmitted by the filter to the diode. An effective means of improving this pass-band performance is to use a photonic crystal with a $L/2H(LH)^4$ structure, instead of the $(LH)^5$ structure. Implementing this requires the last L layer of a $(LH)^5$ structure to be modified, reducing it to one half its original thickness. This modified layer is referred to as an anti-reflection coating (ARC). Another option is to use SiON to form the ARC layer. In this case the SiON is engineered to have $n_{SiON} = 1.85$. This minimizes the reflectance in the pass band.

The reflectance of both the photonic crystal with the SiO_2 ARC and the SiON ARC is shown in Fig. 3(a), where both simulations assumed ideal dielectric constants without losses. Although the Si/SiO_2 photonic crystal exhibits a very flat pass band, the reflectance never goes below 4%. This is due to the refractive index mismatch between the photonic crystal layers and the substrate. In order to achieve zero reflectance—at a discrete set of nulls in the pass-band range—the quarter-wave stack must satisfy the condition[10]

$$\left(\frac{n_2}{n_1}\right)^2 = \frac{n_s}{n_0}. \tag{10}$$

This condition is not satisfied in a Si/SiO_2 photonic crystal deposited on either a Si or GaSb substrate. However, this condition can be satisfied by using a Si/SiON material system to fabricate the 1D photonic crystal filter, where the refractive index of the SiON is engineered to be $n_{SiON} = 1.85$ (assuming the structure is deposited on a Si substrate).

SiON is a useful candidate material for fabricating 1D photonic crystal filters since its refractive index can be varied from 1.5 to 2.0, thus allowing the material pair to be customized to achieve zero reflectance (at a number of discrete frequencies) when used with various substrate materials, resulting in better transmittance over the entire pass band.[11] The reflectance of a Si/SiON photonic crystal is given in Fig. 3(b). This structure exhibits much lower reflectance in the pass band compared to the Si/SiO_2 pair, however, due to lower index contrast between Si and SiON, the filter's stop band is narrower. To quantify the performance of the three different photonic crystal designs detailed above, the Si/SiO_2 stack with a SiO_2 ARC, the Si/SiO_2 stack with a SiON ARC, and the Si/SiON structure, the TPV system efficiency and power density as functions of source temperature (assuming GaSb PV diode) were calculated for each. The results of these calculations are shown in Fig. 4.

The simulation results—presented in Fig. 4—show that the TPV system incorporating a Si/SiON photonic crystal has the highest power density. This is expected given the filter has the lowest pass-band reflectance. However, the Si/SiON 1D photonic crystal filter suffers from lower efficiency due to its narrow stop band. The Si/SiO_2 structure, with a SiO_2 ARC exhibits an almost identical power density to the Si/SiO_2 structure with a SiON ARC. However, the Si/SiO_2 structure with the SiO_2 ARC has superior efficiency.

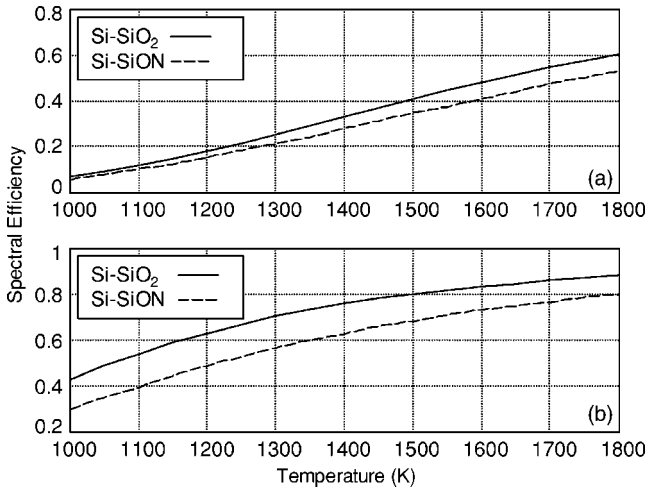

FIG. 5. Simulated spectral efficiencies of Si/SiO_2 $L/2H(LH)^4$ and Si/SiON $L/2H(LH)^4$ photonic crystals for diodes with: (a) $\lambda_{gap}=1.78$ μm (GaSb) and (b) $\lambda_{gap}=2.4$ μm (InGaAsSb).

Therefore, the Si/SiO_2 with a SiO_2 ARC appears to be the best trade-off between efficiency and power density. If power density is of paramount concern the Si/SiON 1D photonic crystal filter is the best option, particularly if it is coupled to a plasma filter, which extends the overall high-reflectance band.

As mentioned earlier, spectral efficiency is another commonly used metric to quantify the performance of a 1D photonic crystal filter in the context of a TPV system. The simulated spectral efficiencies versus temperature of the Si/SiO_2 and Si/SiON photonic crystal filters with the $L/2H(LH)^4$ structure, and designed for use with two PV diode material systems, namely GaSb and InGaAsSb, are shown in Fig. 5. The results of these spectral efficiency simulations suggest that the Si/SiO_2 photonic crystal filter exhibits much better performance than the Si/SiON structure. In addition, it is interesting to note that a Si/SiO_2 photonic crystal designed for use with an InGaAsSb diode has up to 35% higher spectral efficiency than a filter based on the same material system designed for use with a GaSb diode. This difference in performance is due to the large dependence of the filter's spectral efficiency on the electronic band gap of the diode.

IV. FABRICATION OF 1D PHOTONIC CRYSTAL

To experimentally verify the simulation results discussed in the previous sections, a ten-layer Si/SiO_2 $L/2H(LH)^4$ photonic crystal filter was fabricated. This structure was fabricated in accordance with the specifications set out in Sec. III. We used *p*-type Si wafers, and a LPCVD-based process. In order to fabricate the structures such that their physical characteristics actually mirrored the specifications, it was imperative to develop a deposition process that allowed for very accurate and uniform layer deposition. Furthermore, this process needed to have a relatively low thermal budget, given that in the TPV system context the spectral control structure would be directly deposited on the front side of a GaSb photodiode whose device integrity could not be compromised by the filter fabrication process.

The process which was developed to deposit the 1D photonic crystal involved three steps for the deposition of one Si/SiO_2 pair. These three steps were then repeated five times to produce a complete $(LH)^5$ structure. The first step in the process was the deposition of a poly-Si layer. This layer was grown at 625 °C with a SiH_4 flow rate of 150 sccm and a pressure of 200 mTorr. This was followed by the deposition of a low-temperature oxide (LTO) layer, deposited at 400 °C with SiH_4 and O_2 flow rates of 125 and 175 sccm, respectively, at 200 mTorr pressure. The final step in the process was a relatively low-temperature densification anneal at 650 °C for 3 h in a N_2 ambient.

The LPCVD system used had nominal deposition rates for poly-Si and SiO_2 of 10 and 5 nm/min, respectively. A comprehensive set of calibrating deposition runs was carried out prior to the actual photonic crystal fabrication. These runs identified the actual deposition rates as being equal to 10 and 6 nm/min, respectively. The calibration process also identified the effects of the 3 h anneal on the Si/SiO_2 pair. Specifically a 174-nm-thick poly-Si layer was deposited on a high quality thermal oxide (all thickness measurements were taken using a KLA-Tencor UV-1280 Prometrix Thin Film Thickness Measurement System). A 411-nm-thick layer of SiO_2 was then deposited on top and the dielectric pair was annealed at the stated conditions. After the anneal step the thickness of the Si layer was recorded as being 167 nm and that of the SiO_2 as being 353 nm. These results indicated that the Si layer lost 7 nm to oxidation during the anneal, adding 16 nm to the SiO_2 thickness. This meant that the anneal caused an actual reduction in the thickness of the SiO_2 layer of 74 nm. Using this data it was established that in order to ensure that the thickness of the Si and SiO_2 layers was 170 and 390 nm, respectively, after all the processing steps were completed, it was necessary to deposit 177 nm of Si and 456 nm of SiO_2. To produce the final $(LH)^5$ structure the three step process described above was repeated five times.

To fabricate the SiO_2 ARC, the surface layer of the Si/SiO_2 $(LH)^5$ structure was etched, producing the required $L/2H(LH)^4$ structure. The Applied Materials Precision 5000 etcher used a CF_4, CHF_3 chemistry and etched the annealed low-temperature oxide surface layer at a rate of 2 nm/s. Figure 6 shows a transmission electron microscopy (TEM) cross section of the resulting $L/2H(LH)^4$ structure. The lighter strata represent the deposited poly-Si and the darker strata represent the deposited SiO_2. Although from Fig. 6 it can be inferred that Si and SiO_2 layer thicknesses are slightly different from targeted thicknesses (170 and 390 nm, respectively), one should bear in mind that the TEM image was taken at an off-normal angle, thus distorting the true length scale. Indeed, all the calibration measurements that were performed with an ellipsometer (in between deposition steps) proved that the layer thicknesses were well within 5% margin of error.

Furthermore, surface roughness analysis was carried out using an atomic force microscope (Digital Instruments IIIa Nanoscope) in order to be able to quantify scattering losses of the layer interfaces. The Si/SiO_2 interface rms roughness was found to be 4.2 nm for the calibration sample. The surface roughness rms figures for completed filters varied be-

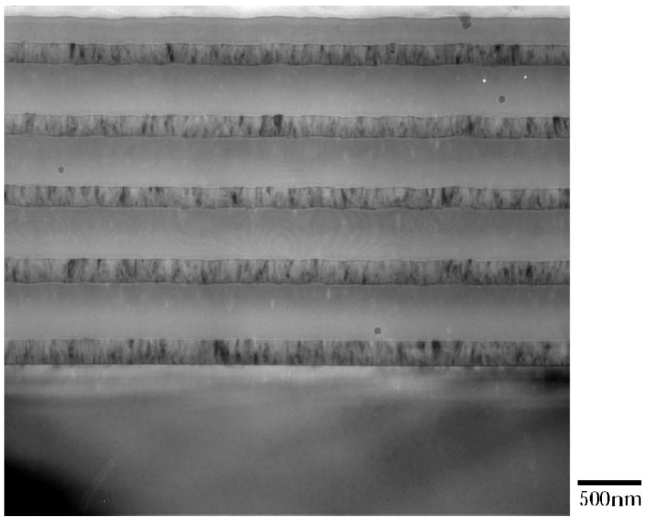

FIG. 6. TEM cross section of Si/SiO_2 1D photonic crystal with SiO_2 ARC. Note Si and SiO_2 layers appear to have slightly different thicknesses from targeted thicknesses (170 and 390 nm, respectively) since the image was taken at an off-normal angle, thus distorting the true image scale.

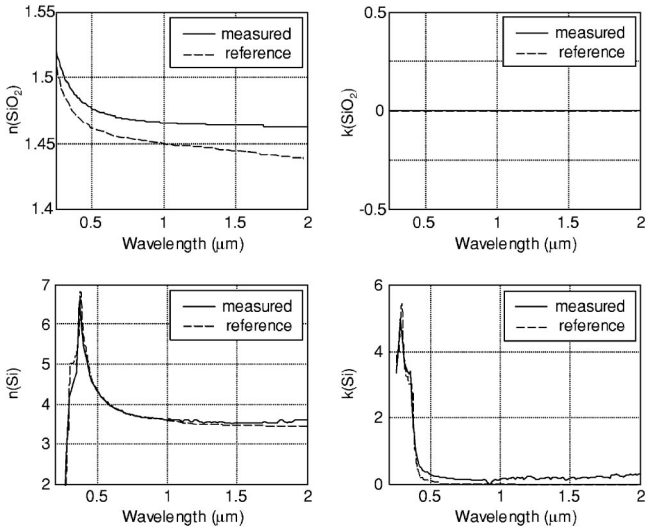

FIG. 7. Measured and Ref. 11 values of the complex refractive indices of Si and SiO_2.

tween 6 and 9 nm—an order of magnitude lower compared to the stack layer thickness—and therefore it was assumed that the scattering due to surface roughness can be neglected.

V. SPECTRAL PERFORMANCE CHARACTERIZATION

The spectral characteristics of the 1D Si/SiO_2 photonic crystal filter, whose design and fabrication are described in the previous section, were measured and compared to the simulated spectral performance. In these tests the reflectance characteristics of the 1D photonic crystal filter, which was deposited on a Si substrate, were measured at both normal and grazing angles of incidence using a Varian Cary 5E spectrophotometer. The measurements were taken over a wavelength range of 0.8–3.3 μm for both TE and TM polarizations. The spectral characterization of the fabricated filter at different angles of incidence is very important because the thermal emitter in a TPV system is a broadband omnidirectional source of radiation. Therefore the effectiveness of any filter's pass band and stop band must be characterized over the complete range of incident angles.

It is important to note that as part of the testing the reflectance characterization of the fabricated filter sample was carried out on a filter sample which was deposited on a Si substrate of finite thickness, while the simulation assumes the substrate is of infinite thickness. To deal with this difference, the physical reflectance measurement results were corrected to eliminate the effect caused by backside reflection from the Si substrate of finite thickness. As a result, the corrected measurement results correspond to the results which would have been obtained had the fabricated filter been deposited on a substrate of infinite thickness.

The measured and simulated characteristics of the filter's normal incidence reflectance exhibit very strong correlation, as shown in Fig. 8. The simulations were carried out using the measured optical constants (n and k) of Si and SiO_2, which are plotted in Fig. 7. The slight shift in the pass-band ripple is due to the layer thickness mismatch between the fabricated filter and the simulated structure. However, due to the large index contrast between the deposited layers the overall design is not very sensitive to fabrication inaccuracies such as slightly varying layer thicknesses. The reflectance characteristics of Fig. 9, measured for off-normal angles of incidence, show that the fabricated Si/SiO_2 1D photonic crystal maintains acceptable levels of spectral performance even at incident angle of 50°, preserving both the critical stop- and pass-band characteristics.

In order to estimate TPV system power density and efficiency as well as the filter's own spectral efficiency and in-band transmission, the measured reflectance and transmittance data were employed. Power density was estimated using Eq. (4), diode efficiency was estimated using Eq. (5), spectral efficiency was estimated using Eq. (6). In-band transmission ($T_{>\omega_g}$) is defined as the ratio of transmitted power above the band gap energy to the total emitted power above the band gap. Results for in-band transmission for different emitter temperatures (for a blackbody radiation source) are given in Table I. The estimated diode efficiency at 1500 K source temperature is 24% with a power density of 2.1 (W/cm^2) and a filter spectral efficiency of 40%. These results indicate that in terms of "integral" performance measures (η_{TPV}, P_{PV}, $\eta_{spectral}$, $T_{>\omega_g}$) the fabricated filter performs nearly as well as the simulated filter with ideal parameters. The filter's in-band transmission results in 65% of the convertible thermal power reaching the diode. Although one would expect better in-band transmission—especially judging from the normal incidence reflectance data in Fig. 8—it

TABLE I. Estimated TPV system efficiency, power density, filter spectral efficiency and integrated in-band transmittance using measured filter data.

T_{BB} (K)	η_{TPV} (%)	P_{PV} (W/cm^2)	$\eta_{spectral}$ (%)	$T_{>\omega_g}$ (%)
1300	15	0.7	26	65
1400	19	1.2	33	65
1500	24	2.1	40	65

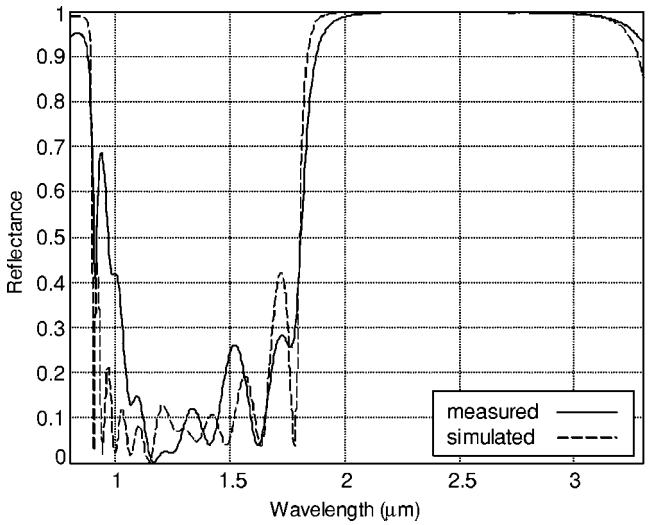

FIG. 8. Measured and simulated normal incidence reflectance characteristic of $L/2H(LH)^4$ 1D Si/SiO_2 photonic crystal filter.

must be realized that the overall filter transmission is an angle-weighted average transmission, as given in Eq. (3).

VI. OVERVIEW AND CONCLUSION

It has been widely acknowledged that the goal of developing TPV systems that meet critical performance benchmarks in terms of efficiency and power density relies heavily on the effectiveness of the system's spectral control components. In this article we have focused on the design, optimization, fabrication and characterization of a Si/SiO_2 1D photonic crystal for use as such a spectral control component.

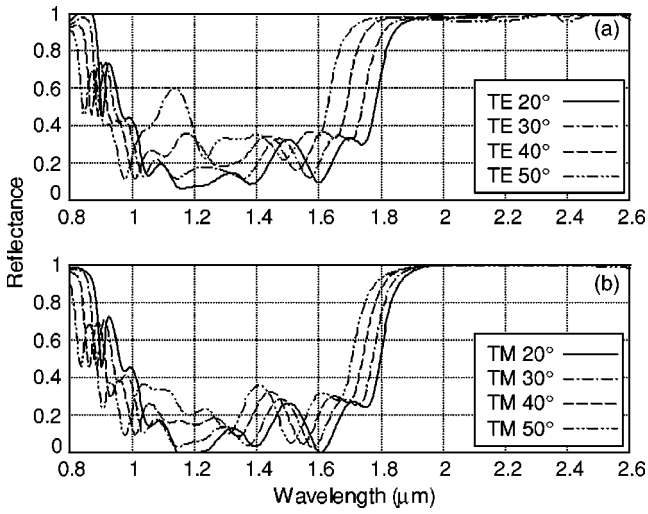

FIG. 9. Measured reflectance characteristics of $L/2H(LH)^4$ 1D Si/SiO_2 photonic crystal filter at 20°, 30°, 40° and 50° incidence for both TE and TM polarizations.

We have shown that large index contrast material systems like Si/SiO_2 provide a large omnidirectional stop band while at the same time have a wide pass band and low absorption losses—thus satisfying the key requirements for insuring high efficiency and high power density within the TPV context. In this article we fully describe the LPCVD fabrication process using standard microfabrication techniques, which was developed to fabricate the Si/SiO_2 photonic crystals. Measurements of the optical constants of the LPCVD deposited Si and SiO_2 showed excellent agreement with the reference values of their crystalline counterparts. The characterization of the fabricated samples proved that the fabrication process provided excellent control of the filter's design parameters, including layer thicknesses, surface roughness, and a high level of repeatability. The reflectance and transmittance spectral characterization of the fabricated Si/SiO_2 1D photonic crystals confirmed that the physical sample's spectral characteristics conformed with what simulations of the structure's spectral characteristics had predicted. Ultimately a filter with a 40% spectral efficiency at 1500 K blackbody emitter temperature was fabricated, using techniques that are easily adapted to large scale deposition of filters on the front side of TPV system PV cells.

The results presented in this article substantiate the claims made at the beginning of this article that Si/SiO_2 1D photonic crystals can be used as inexpensive, practical, high-performance front-side spectral control components within a TPV context.

ACKNOWLEDGMENTS

The authors wish to thank Professor David Perreault, Dr. Thomas Keim, David Danielson and Professor Lionel Kimerling of MIT for numerous discussions and valuable suggestions during the course of this work and in the final phase of the manuscript preparation. This work was sponsored by MIT/Industry Consortium on advanced Automotive Electrical/Electronic Components and Systems.

[1] P. Aigrain, *The Thermophotovoltaic Converter* (unpublished lectures given at MIT, 1960).
[2] R. E. Black, P. F. Baldasaro, and G. W. Charache, 18th International Conference on Thermoelectrics, 1999, pp. 639–644.
[3] Y. Fink, J. Winn, S. Fan, C. Chen, J. Michael, J. Joannopoulos, and E. Thomas, Science **282**, 1679 (1998).
[4] R. Almeida and Z. Wang, Proc. SPIE **4655**, 24 (2002).
[5] M. Patrini, M. Galli, M. Belotti, L. Andreani, and G. Guizzetti, J. Appl. Phys. **92**, 1816 (2002).
[6] M. Zenker, A. Heinzel, G. Stollwerck, J. Ferber, and J. Luther, IEEE Trans. Electron Devices **48**, 367 (2001).
[7] I. Celanovic, F. O'Sullivan, M. Ilak, J. Kassakian, and D. Perreault, Opt. Lett. **29**, 863 (2004).
[8] J. N. Winn, Y. Fink, S. Fan, and J. D. Joannopoulos, Opt. Lett. **23**, 1573 (1998).
[9] P. Yeh, *Optical Waves in Layered Media* (Wiley, New York, 1988).
[10] E. Hecht, *Optics* (Addison–Wesley, San Francisco, 2002).
[11] E. D. Palik, *Handbook of Optical Constants of Solids* (Academic, New York, 1985).